

Chiral eigenbases of the XX and XY quantum spin chains

Xin Zhang,¹ Frank Göhmann,² Andreas Klümper,² and Vladislav Popkov^{2,3}

¹*Beijing National Laboratory for Condensed Matter Physics,*

Institute of Physics, Chinese Academy of Sciences, Beijing 100190, China

²*Department of Physics, University of Wuppertal, Gausstraße 20, 42119 Wuppertal, Germany*

³*Faculty of Mathematics and Physics, University of Ljubljana, Jadranska 19, SI-1000 Ljubljana, Slovenia*

We calculate the values of observables in chiral eigenstates of the XX quantum spin chain that were introduced in previous work and compare the form of the result with the respective expressions obtained in the more familiar eigenbasis of states with fixed magnetization in z -direction. We carry out the diagonalization of the XY spin chain in the chiral basis. We calculate the norm of the chiral XY eigenstates, and the values of the one-point functions and some neighbor two-point correlation functions. We interpret the spectrum and the particle content of the XY chain in terms of scattering states of an even number of kink and anti-kink excitations that are created over a reduced Brillouin zone.

Introduction— Chiral quantum states with nontrivial topology are becoming an important tool in quantum technologies. With atoms in optical lattices it is possible to pass from non-interacting to strongly correlated spin states by adiabatic manipulations in external electromagnetic fields [8, 26, 27]. The nontrivial topology of chiral eigenstates entails their exceptional robustness against noise even compared to the ground state [15]. It appears therefore natural to describe generic chiral states (not necessarily eigenstates) and their time evolution not in terms of the conventional computational basis (which is topologically trivial), but rather in terms of a basis which is chiral and topologically nontrivial by itself. A chiral basis for qubits was proposed in [19], where it was employed to study the relaxation of spin helix states in the XX chain. This chiral basis shares all the convenient features of the computational basis, such as the product structure and orthonormality, but at the same time is intrinsically topological, as will be seen below.

The convenience of the chiral basis can be illustrated with a simple example: let us take a spin helix state

$$|\Phi(\alpha, \eta)\rangle = \bigotimes_n \frac{1}{\sqrt{2}} \begin{pmatrix} 1 \\ e^{i(\alpha+n\eta)} \end{pmatrix}, \quad \alpha, \eta \in \mathbb{R}, \quad (1)$$

where $\begin{pmatrix} 1 \\ e^{i\eta} \end{pmatrix}$ describes the state of a qubit, while $+n\eta$ represents a linear increase of the qubit phase along the chain. The qubit polarization along the chain forms a helix of period $2\pi/\eta$ in the xy -plane. A shift of the initial phase α in (1) does not affect the physical properties of the helix. However, representing such a phase shift in the computational basis is inconvenient: it will affect all the terms of the expansion in different manners. On the contrary, the chiral qubit basis [19] allows to accommodate the phase α by a global rotation about the z -axis.

In this work we intend to demonstrate that the practical usage of a chiral qubit basis can be as simple as the usage of the computational basis of S^z eigenstates. This is true, in particular, in connection with the XX quantum spin chain [17] that can be diagonalized in either basis as the Hamiltonian commutes with the operator of the z -component of the total spin S^z as well as with a winding number operator V [19] (see (7) below) that measures the chirality in the xy -plane. This means that the XX Hamiltonian is block diagonal in both bases, with blocks that either have fixed values of the total magnetization in z -direction or fixed winding numbers in the xy -plane. Both block structures are, however, incompatible as S^z and V do not commute. For this reason, the magnetization in z -direction and the winding number cannot be measured simultaneously.

In both eigenbases the eigenfunctions of the XX Hamiltonian are parametrized in terms of quasimomenta, or Bethe roots, that satisfy simple Bethe equations. Although the Bethe equations are of similar form in both cases, the meaning of the usual quasimomenta k_j in the S^z eigenbasis and the quasimomenta p_j in the chiral basis is different. In particular, simple spectral observables and expectation values of one-point and neighbor two-point correlation functions are not necessarily expressed the same way in both types of quasimomenta. We shall discuss a number of examples below.

In the second part of our manuscript we diagonalize the anisotropic XY Hamiltonian H_{XY} in the chiral basis. H_{XY} is not rotation invariant and does not commute with S^z . Still, it commutes with the winding number operator V that provides a $U(1)$ symmetry and a block structure in this case. The XY model was introduced and solved, by mapping it to a model of non-interacting Fermions, in the seminal work [17] of Lieb, Schultz and Mattis. For this model Bethe Ansatz solutions other than those that can be obtained as special cases from Bethe Ansatz solutions of the more general XYZ chain are not available. For the XYZ chain a coordinate Bethe Ansatz solution was obtained by Baxter [2–4], and algebraic versions are due to Takhtadjan and Faddeev [25] (see also [16, 23]) and to Felder and Varchenko [9]. These solutions have in common that they diagonalize the transfer matrix of the underlying eight-vertex model which does not commute with the winding number operator V . Recently, three of the authors proposed a new variant

of the coordinate Bethe Ansatz for the XYZ chain [30] that applies to the XYZ Hamiltonian, but not to the transfer matrix. As we shall see, the XY limit of this Bethe Ansatz solution gives a chiral orthonormal eigenbasis of the model. The eigenfunctions inherit their parametrization in terms of rapidity variables from the XYZ chain. They take the form of determinants with entries that are elliptic functions. We also provide a reparametrization in terms of quasimomenta. In terms of these the eigenfunctions take a particularly simple form and allow us to interpret the elementary excitation of the finite chain as kink-anti-kink pairs living in a reduced Brillouin zone. We finally provide explicit expressions of some simple observables in terms of the quasimomenta.

I. XX MODEL: S^z VERSUS CHIRAL EIGENBASIS

The one-dimensional periodic spin- $\frac{1}{2}$ XX model is defined by the Hamiltonian

$$H_{XX} = \sum_{n=1}^N (\sigma_n^x \sigma_{n+1}^x + \sigma_n^y \sigma_{n+1}^y), \quad \sigma_{N+1}^\alpha \equiv \sigma_1^\alpha, \quad (2)$$

where σ_n^α , $\alpha = x, y, z$, act as Pauli matrices on the n th spin in the chain and where we set the exchange parameter equal to 1. The XX model is among the simplest exactly solvable many-body systems. Its solvability can be attributed to the fact that it can be mapped to a model of non-interacting Fermions by a Jordan-Wigner transformation [17]. Alternatively, the model can be related to the six-vertex model [1, 24] at the free Fermion point. Within this interpretation the Hamiltonian is proportional to the logarithmic derivative of the six-vertex model transfer matrix. Its spectrum and eigenfunctions can therefore be obtained by means of the algebraic Bethe Ansatz [22]. For the application of the latter method it is crucial that the transfer matrix (and hence the Hamiltonian) commutes with the operator

$$S^z = \frac{1}{2} \sum_{n=1}^N \sigma_n^z \quad (3)$$

of the z -component of the total spin.

Let $|\uparrow\rangle_z = \begin{pmatrix} 1 \\ 0 \end{pmatrix}$ and $|\downarrow\rangle_z = \begin{pmatrix} 0 \\ 1 \end{pmatrix}$ be normalized eigenvectors of σ^z with eigenvalues ± 1 . Then the states

$$|s_1 s_2 \dots s_N\rangle_z = |s_1\rangle_z \otimes |s_2\rangle_z \otimes \dots \otimes |s_N\rangle_z \quad (4)$$

with $s_j \in \{\uparrow, \downarrow\}$ form a basis of eigenstates of S^z on the space of states $\mathcal{H}_N = (\mathbb{C}^2)^{\otimes N}$ of the XX Hamiltonian (2). Since $[H_{XX}, S^z] = 0$, the Hamiltonian (2) is block diagonal in this basis, and the blocks can be labeled by the eigenvalues $-N/2, -N/2+1, \dots, N/2$ of S^z . A state with m \uparrow -spins and $N-m$ \downarrow -spins corresponds to an S^z eigenvalue of $m - N/2$. Clearly, the number of such states is $\binom{N}{m}$. An efficient way to address these states is to specify the positions of \uparrow -spins on a background of \downarrow -spins. For this purpose choose m integers n_j , $1 \leq n_1 < n_2 < \dots < n_m \leq N$ and set $\mathbf{n} = (n_1, \dots, n_m)$ and $|\mathbf{n}\rangle_z = \sigma_{n_1}^+ \dots \sigma_{n_m}^+ |\downarrow \dots \downarrow\rangle_z$. The entirety of such states for fixed m is a basis of the $\langle S^z \rangle = m - N/2$ subspace of \mathcal{H}_N .

Theorem 1. [See e.g. [7]]. For $m = 1, 2, \dots, N$, define $\mathbf{k} = (k_1, k_2, \dots, k_m)$, $k_j \in (-\pi, \pi]$ with $k_1 < \dots < k_m$. The states

$$|\xi_m(\mathbf{k})\rangle = \sum_{1 \leq n_1 < \dots < n_m \leq N} \chi_{\mathbf{n}}(\mathbf{k}) |\mathbf{n}\rangle_z, \quad \chi_{\mathbf{n}}(\mathbf{k}) = \frac{1}{\sqrt{N^m}} \det_{j,l=1,\dots,m} \{e^{ik_j n_l}\}, \quad (5)$$

where the quasi-momenta k_j satisfy the Bethe equations $e^{iNk_j} = (-1)^{m-1}$, together with the pseudo vacuum $|\downarrow \dots \downarrow\rangle_z$, form a complete set of mutually orthogonal, normalized eigenstates of the Hamiltonian (2). The corresponding energy eigenvalues are

$$E(\mathbf{k}) = 4 \sum_{j=1}^m \cos k_j. \quad (6)$$

We call the basis $\{|\xi_m(\mathbf{k})\rangle\}$ the S^z eigenbasis of the XX Hamiltonian (2). It is of appealing simplicity as the wave function within the blocks of fixed S^z eigenvalues take the form of Slater determinants.

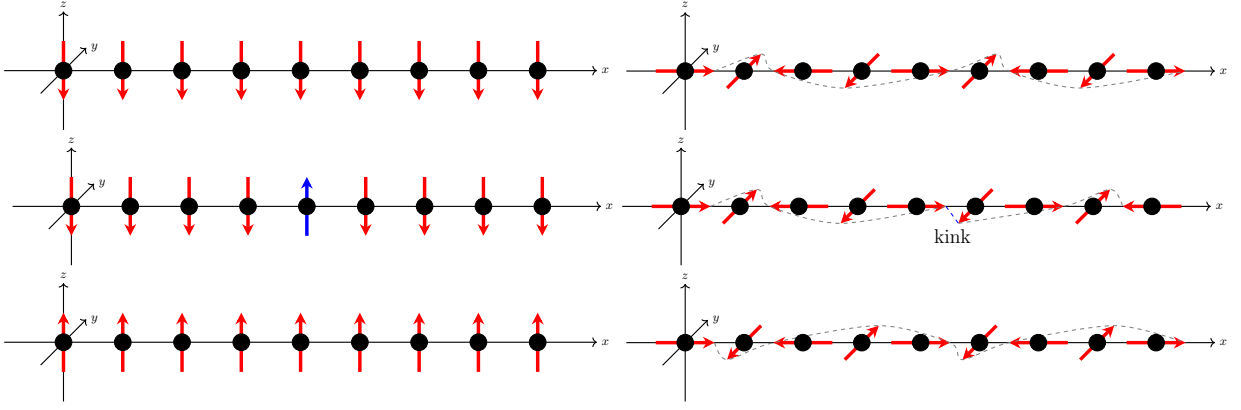


FIG. 1. Visualization of the conventional S^z basis and the chiral basis. **Left panel:** From top to bottom, the states are the all spin-down state $|\emptyset\rangle_z$, the one spin-flip state $|n_1\rangle_z$, and the all spin-up state $|1, 2, \dots, N\rangle_z$. **Right panel:** From top to bottom, the spin-helix state $|1; \emptyset\rangle$, the one kink state $|1; n_1\rangle$, and another spin-helix state with different chirality $|1; 1, 2, \dots, N\rangle$.

In Ref. [19] we constructed another rather different eigenbasis of the XX Hamiltonian, the chiral eigenbasis, which is almost as simple as the S^z eigenbasis. The chiral basis is a basis of joint eigenvectors of H_{XX} and the operator

$$V = \frac{1}{4} \sum_{l=1}^{N/2} (\sigma_{2l-1}^x \sigma_{2l}^y - \sigma_{2l}^y \sigma_{2l+1}^x), \quad (7)$$

whose commutativity with H_{XX} follows from its commutativity with the more general XY Hamiltonian which is proved in App. B. Like the eigenstates of S^z , all eigenstates of V can be chosen as tensor products of eigenstates of Pauli matrices. All states

$$|\kappa; \mathbf{n}\rangle = (-i)^{\sum_{j=1}^M n_j} \bigotimes_{l=1}^{n_1} \psi(l - \kappa) \bigotimes_{l=n_1+1}^{n_2} \psi(l - 2 - \kappa) \cdots \bigotimes_{l=n_M+1}^N \psi(l - 2M - \kappa), \quad \psi(u) = \frac{1}{\sqrt{2}} \begin{pmatrix} 1 \\ i^u \end{pmatrix}, \quad (8)$$

where $\kappa = \pm 1$, $\mathbf{n} = (n_1, \dots, n_M)$, $1 \leq n_1 < n_2 < \dots < n_M \leq N$, are eigenstates of V and form an orthonormal basis of \mathcal{H}_N which we call the chiral basis. In such states the qubit polarization changes from factor to factor by an angle of $+\pi/2$ or $-\pi/2$ in the xy -plane. Each anticlockwise or clockwise rotation by $\pi/2$ adds $+\frac{1}{4}$ or $-\frac{1}{4}$ to the eigenvalue of V so that

$$V|\kappa; \mathbf{n}\rangle = \frac{1}{4}(N - 2M)|\kappa; \mathbf{n}\rangle, \quad \kappa = \pm 1, \quad (9)$$

where M is the number of clockwise rotations, further referred to as *kinks*. We say a kink is located at n_j if the rotation between site n_j and site n_{j+1} is clockwise. Each state (8) is uniquely characterized by its kink positions \mathbf{n} and the polarization of the first qubit, where $\kappa = +1, -1$ correspond to the eigenstates of σ^x with eigenvalues $+1$ and -1 respectively.

The state $|-1; \mathbf{n}\rangle$ is obtained from $|1; \mathbf{n}\rangle$ by a simultaneous inversion of all spins in the xy -plane. Such an inversion preserves the number and the locations of kinks and results in a linearly independent eigenstate of V with the same eigenvalue. The states with no kinks, in which the phase winds anticlockwise from every site to the next, play the role of the “pseudo vacua” for the chiral basis. We shall denote them by $|\kappa; \emptyset\rangle$, $\kappa = \pm 1$. For a visualization of the eigenstates of V and of S^z see Fig. 1.

The operator V counts the number of rotations of the polarization in the xy -plane in a basis state (8). For this reason we call it the winding number operator and its eigenvalue the winding number. The XX Hamiltonian H_{XX} commutes with the winding number operator V , if the number of lattice sites N is even. Hence, on lattices with an even number of sites, H_{XX} can be diagonalized at fixed winding number. For compatibility with periodic boundary conditions the winding number must be an integer, implying that M must have the same parity as $N/2$. Such values of M , odd integers for $N/2$ odd and even integers for $N/2$ even, will be called admissible.

Theorem 2. [19]. For $M = 1, 2, \dots, N$ define $\mathbf{p} = (p_1, p_2, \dots, p_M)$, $p_j \in (-\pi, \pi]$ with $p_1 < \dots < p_M$. The states

$$|\mu_M(\mathbf{p})\rangle = \sum_{1 \leq n_1 < \dots < n_M \leq N} \sum_{\kappa = \pm 1} \chi_{\mathbf{n}}(\mathbf{p}) \kappa^\xi |\kappa; \mathbf{n}\rangle, \quad \xi = 0, 1, \quad \chi_{\mathbf{n}}(\mathbf{p}) = \frac{1}{\sqrt{2^N M}} \det_{j,l=1,\dots,M} \{e^{ip_j n_l}\}, \quad (10)$$

Operator of an observable/conserved quantity \hat{A}	S^z eigenstate expectation $\langle \hat{A} \rangle_{\mathbf{k}}$	Chiral eigenstate expectation $\langle \hat{A} \rangle_{\mathbf{p}}$
transversal magnetization	0	0
$\sigma_{j_1}^{\alpha_1} \sigma_{j_2}^{\alpha_2} \dots \sigma_{j_{2k+1}}^{\alpha_{2k+1}}, \alpha_l = x, y$	0	0
$S^z = \frac{1}{2} \sum_l \sigma_l^z$	$m - N/2$	$\sum_{j=1}^M \sin p_j$
winding number V	$\frac{1}{2} \sum_{j=1}^m \sin k_j$	$\frac{1}{4}(N - 2M)$
energy	$4 \sum_{j=1}^m \cos k_j$	$4 \sum_{j=1}^M \cos p_j$
momentum $(-i \ln T)$	$\sum_{j=1}^m k_j$	—
“double” momentum $(-i \ln T^2)$	$2 \sum_{j=1}^m k_j$	$2 \sum_{j=1}^M p_j + (M + \xi)\pi$
total magnetization current $J = \sum_l j_l$	$8 \sum_{j=1}^m \sin k_j$	$2N \left(1 - \frac{4}{N} \sum_{j=1}^M \sin^2 p_j\right)$

TABLE I. Comparison of observables and conserved quantities $\langle \hat{A} \rangle_{\mathbf{k}}$ and $\langle \hat{A} \rangle_{\mathbf{p}}$ for the S^z and chiral eigenstates of the XX model.

where M is admissible and the chiral quasi-momenta p_j satisfy $e^{iNp_j} = (-1)^{\xi+1}$ for all p_j , form a complete set of mutually orthogonal, normalized eigenstates of the Hamiltonian (2). The corresponding eigenvalues are

$$E(\mathbf{p}) = 4 \sum_{j=1}^M \cos p_j. \quad (11)$$

We call the basis $\{\mu_M(\mathbf{p})\}$ the chiral eigenbasis of the XX Hamiltonian (2). It is of the same appealing simplicity as the S^z eigenbasis in Thm. 1.

Unlike the basis of S^z eigenvectors (4) (where a local flip of any spin in vertical direction changes the z -magnetization by one unit), the chiral basis vectors (8) have a topological nature: a single kink cannot be added to (removed from) a periodic chain by any local operatorial action. In an open chain this is only possible at the boundaries. Thus, the sectors with different chiralities $M, M \pm 1$ are topologically protected.

Note that $[H_{XX}, S^z] = [H_{XX}, V] = 0$, but $[V, S^z] \neq 0$. The two families of XX eigenstates, given by the Theorems 1 and 2 are different. This is possible due to the large degeneracy of the eigenstates of the Hamiltonian. Still, some important eigenstates are non-degenerate, for instance, the ground state. Within both eigenbases (S^z and chiral) the ground state is constructed by filling a Fermi sea with quasiparticles that add negative contributions to the energy ($\cos k_j < 0$ in the S^z eigenbasis, or $\cos p_j < 0$ in the chiral eigenbasis). It can be easily seen that for an XX chain of even length N , the ground state belongs to the intersection of the blocks $m = N/2$ of vanishing magnetization and $M = N/2$ of zero winding number.

II. COMPARISON OF EXPECTATION VALUES OF OBSERVABLES IN S^z AND CHIRAL XX EIGENSTATES

Here we compare one-point and neighbor two-point functions calculated in the eigenstates $|\xi_m(\mathbf{k})\rangle$ and $|\mu_M(\mathbf{p})\rangle$. We shall introduce shorthand notations for the respective expectation values,

$$\langle \hat{A} \rangle_{\mathbf{k}} \equiv \langle \xi_m(\mathbf{k}) | \hat{A} | \xi_m(\mathbf{k}) \rangle \quad (12)$$

in sectors of fixed magnetization and

$$\langle \hat{A} \rangle_{\mathbf{p}} \equiv \langle \mu_M(\mathbf{p}) | \hat{A} | \mu_M(\mathbf{p}) \rangle \quad (13)$$

for fixed winding number. The results are summarized in Tab. I.

We are denoting the translation operator by T . Note that $[H_{XX}, T] = 0$, but $[V, T] \neq 0$. We rather have $[V, T^2] = 0$. Hence, the usual momentum is not a good quantum number for chiral eigenstates. We shall further discuss this below, when we are discussing the elementary excitation of the more general XY chain.

The conserved magnetization current in z -direction will be denoted J . Its density is

$$j_l = 2(\sigma_l^x \sigma_{l+1}^y - \sigma_l^y \sigma_{l+1}^x). \quad (14)$$

We can express it as $J = 8(V + TVT^{-1})$. The vectors in the S^z eigenbasis are joint eigenvectors of H_{XX} , S^z and T , implying that $\langle J \rangle_{\mathbf{k}} = 8\langle (V + TVT^{-1}) \rangle_{\mathbf{k}} = 16\langle V \rangle_{\mathbf{k}}$.

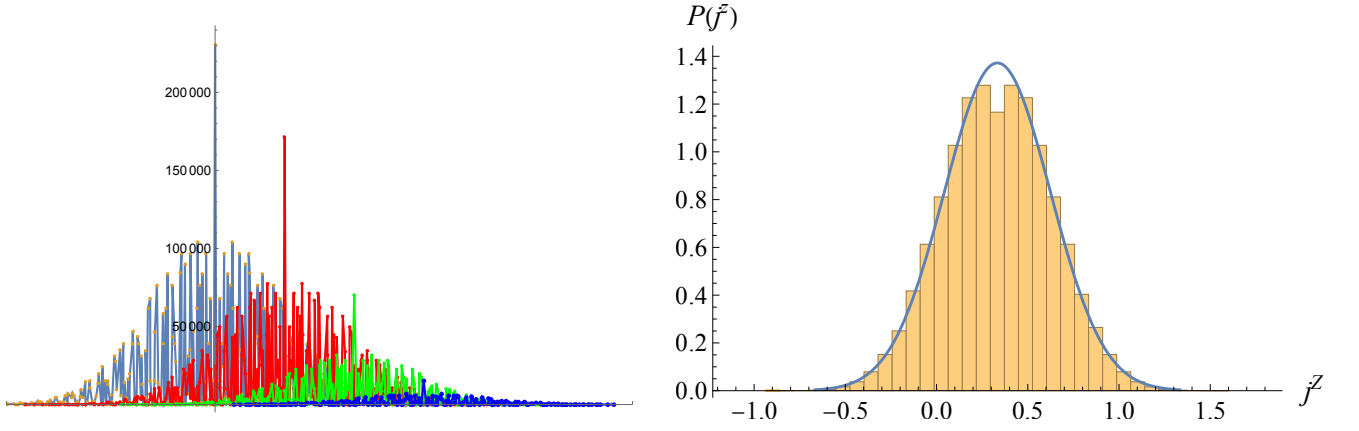


FIG. 2. **Left Panel:** Cumulative frequency distribution (total number of appearances) of the z -magnetization current of the XX eigenstates inside chiral blocks for a system of size $N = 24$. Light blue, red, green, blue peaks belong to chiral blocks $M = 12, 10, 8, 6$ respectively. The currents' arrangement is symmetric with respect to the central peak, located at $\langle j_i \rangle = 2(1 - \frac{2M}{N})$, according to Eq. (16). The currents for $M > N/2$ (not shown) are located symmetrically on the left side. **Right Panel:** Probability density distribution of the currents in the red block of the left Panel. A Gaussian blue curve with exact variance $\sigma = \sqrt{35/414} \approx 0.29$ calculated from (17) is a guide to the eye.

To get a better understanding of the difference of the expectation values in the two bases, let us consider averages and distributions of currents within blocks of fixed magnetization and of fixed winding number. The average of the total current within any block of fixed S^z is zero, since the current is an odd function of the symmetrically distributed quasimomenta k_j . Indeed, for the XX eigenfunctions $|\xi_m(\mathbf{k})\rangle$ (5) from Theorem 1 obtained via the usual computational basis, i.e. within invariant blocks of fixed z -axis magnetization, $(\sum_{j=1}^N \sigma_j^z) |\xi_m(\mathbf{k})\rangle = (2m - N) |\xi_m(\mathbf{k})\rangle$, $m = 0, 1, 2, \dots, N$, the average current and its variance within the blocks of fixed m are

$$\bar{J}_{\text{fixed } m} = 0, \quad \langle (J - \bar{J})^2 \rangle_m = 32m \frac{1 - \frac{m}{N}}{1 - \frac{1}{N}}. \quad (15)$$

On the contrary, the same average of the total current within chiral blocks for $|\mu_M(\mathbf{p})\rangle$ is generically nonzero (see App. I) as here the current is the sum of an even function of the quasimomenta p_j .

$$\bar{J} = 2(N - 2M) \quad (16)$$

with variance

$$\langle (J - \bar{J})^2 \rangle_M = 8M \frac{1 - \frac{M}{N}}{1 - \frac{1}{N}}. \quad (17)$$

The above result is exact in the thermodynamic limit and numerically appears to be extremely accurate for all M, N . Examples for the asymmetric distribution of the current for different fixed winding numbers are shown in Fig. 2.

III. DIAGONALIZATION OF THE XY MODEL IN THE CHIRAL BASIS

It is straightforward to see (cf. App. B) that the Hamiltonian

$$H_{XY} = \sum_{n=1}^N (J_x \sigma_n^x \sigma_{n+1}^x + J_y \sigma_n^y \sigma_{n+1}^y), \quad \sigma_{N+1}^\alpha \equiv \sigma_1^\alpha, \quad (18)$$

of the XY spin- $\frac{1}{2}$ chain with periodic boundary conditions commutes with the winding number operator V , if N is even. Hence, H_{XY} is block diagonal in the chiral basis. An orthonormal chiral eigenbasis is obtained by taking the XY limit in the coordinate Bethe Ansatz solution [30] of the XYZ chain that was recently obtained by three of the authors (cf. App. C1).

The description of the chiral eigenbasis in terms of rapidity variables below involves the Jacobi theta functions $\theta_j(u, q)$, $j = 1, 2, 3, 4$, [29]. We recall their definition in App. A (for more details see also [18]). For the nome q we employ the parameterization $q = e^{i\pi\tau}$, with $\tau \in \mathbb{C}$, $\text{Im } \tau > 0$. We shall further use the shorthand notations

$$\theta_j(u) \equiv \theta_j(u, e^{i\pi\tau}), \quad \theta'_j(u) \equiv \frac{d\theta_j(u)}{du}, \quad j = 1, 2, 3, 4. \quad (19)$$

Restricting ourselves to real positive values of the exchange constants J_x and J_y in (18) for simplicity, we adopt the parametrization

$$J_x = \frac{\theta_3(0)}{\theta_4(0)}, \quad J_y = \frac{\theta_4(0)}{\theta_3(0)}. \quad (20)$$

Then the following theorem holds.

Theorem 3. *The states*

$$|\Psi_M(\mathbf{u})\rangle = \sum_{1 \leq n_1 < \dots < n_M \leq N} \sum_{\kappa = \pm 1} \chi_{\mathbf{n}}(\mathbf{u}) \kappa^\xi |\kappa; \mathbf{n}\rangle, \quad \xi = 0, 1, \quad (21)$$

$$\chi_{\mathbf{n}}(\mathbf{u}) = \frac{1}{\sqrt{2N^M}} \det_{j,l=1,\dots,M} \{\mathcal{A}_{n_j}(u_l)\}, \quad \mathcal{A}_n(u) = \left[\frac{\theta_1(u + \frac{1}{4})}{\theta_1(u - \frac{1}{4})} \right]^n \left[\frac{\theta_3(u + \frac{\epsilon_n}{4})}{\theta_3(u - \frac{\epsilon_n}{4})} \right]^{\frac{1}{2}}, \quad \epsilon_n = (-1)^n,$$

where M is admissible and the ordered Bethe roots $\mathbf{u} = (u_1, u_2, \dots, u_M)$ satisfy

$$\left[\frac{\theta_1(u_j + \frac{1}{4})}{\theta_1(u_j - \frac{1}{4})} \right]^N = (-1)^{\xi+1}, \quad j = 1, \dots, M, \quad (22)$$

form a complete set of mutually orthogonal, normalized eigenstates of the Hamiltonian (18), (20).

The corresponding eigenvalues of H_{XY} are

$$E(\mathbf{u}) = 2 \frac{\theta_2(0)}{\theta_1(0)} \sum_{j=1}^M \left[\frac{\theta'_1(u_j - \frac{1}{4})}{\theta_1(u_j - \frac{1}{4})} - \frac{\theta'_1(u_j + \frac{1}{4})}{\theta_1(u_j + \frac{1}{4})} \right]. \quad (23)$$

Remark. We consider the Hermitian case, where τ is purely imaginary. Without loss of generality, all Bethe roots are restricted to the rectangles $-\frac{1}{2} < \text{Re } u \leq 0$, $-\frac{\text{Im } \tau}{2} < \text{Im } u \leq \frac{\text{Im } \tau}{2}$ and $0 < \text{Re } u \leq \frac{1}{2}$, $-\frac{\text{Im } \tau}{2} \leq \text{Im } u < \frac{\text{Im } \tau}{2}$. In our elliptic parametrization the Bethe roots $\{u_j\}$ are then distributed along two lines in the complex plane: $\text{Re}(u_j) = 0, \frac{1}{2}$ (cf. App. D).

Remark. Once u_j is a solution of the Bethe Ansatz equations (22), then $u_j + \frac{1}{2}$ is a solution as well. Since u_j and $u_j + \frac{1}{2}$ yield energies of the same absolute values, but with different signs, the complete spectrum of the Hamiltonian is symmetric with respect to sign reversal.

Remark. As in the XY case, our chiral Bethe states are eigenstates of the Hamiltonian but not of the transfer matrix of the underlying eight-vertex model. This distinguishes our approach from the algebraic Bethe Ansatz method [23, 25].

The proof of Thm. 3 is split into three parts: the proof of the commutativity $[H_{XY}, V] = 0$, the proof of the main body of the theorem for unnormalized eigenvectors, and, finally, the proof of the normalization. The three proofs are given in App. C.

The form (22) of the Bethe equations suggests to introduce a “momentum function” p by the equation

$$e^{ip(u)} = \frac{\theta_1(u + \frac{1}{4})}{\theta_1(u - \frac{1}{4})} \quad (24)$$

and to express the eigenvectors and the energy eigenvalues in terms of the quasi-momenta $p_j = p(u_j)$. This is done in App. D and results in the following corollary to Thm. 3.

Corollary 1. *The states*

$$|\tilde{\Psi}_M(\mathbf{p})\rangle = \sum_{1 \leq n_1 < \dots < n_M \leq N} \sum_{\kappa = \pm 1} \tilde{\chi}_{\mathbf{n}}(\mathbf{p}) \kappa^\xi |\kappa; \mathbf{n}\rangle, \quad \xi = 0, 1, \quad \tilde{\chi}_{\mathbf{n}}(\mathbf{p}) = \frac{1}{\sqrt{2N^M}} \det_{j,l=1,\dots,M} \{\tilde{\mathcal{A}}_{n_j}(p_l)\}, \quad (25)$$

$$\tilde{\mathcal{A}}_n(p) = \exp[i(np - \epsilon_n \varphi(p))], \quad \varphi(p) = \frac{1}{2} \arctan \left(\frac{J_x - J_y}{J_x + J_y} \tan p \right), \quad \epsilon_n = (-1)^n,$$

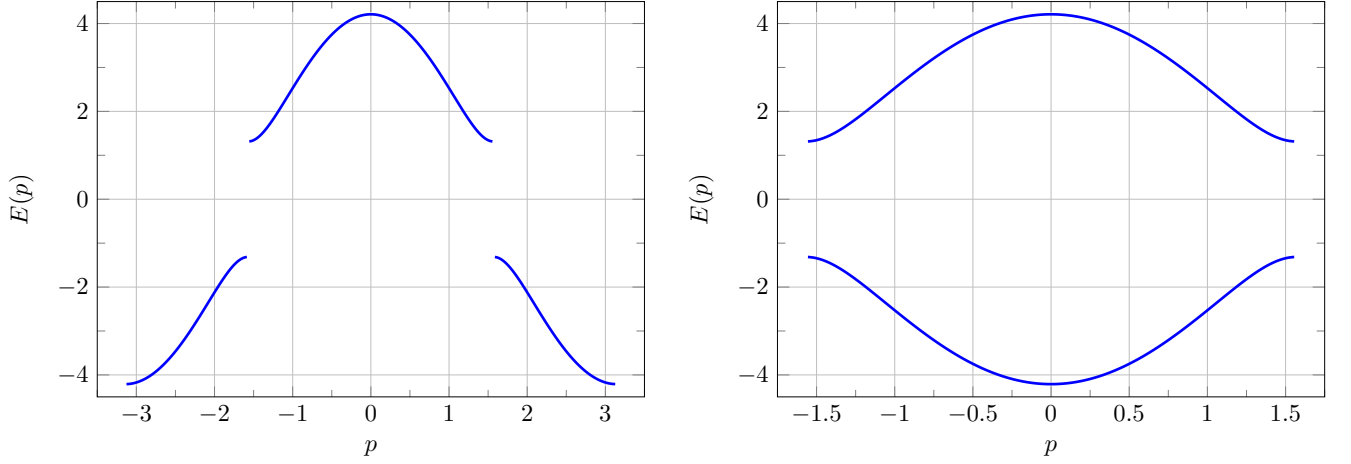


FIG. 3. The dispersion relations in the full Brillouin zone $(-\pi, \pi]$ (left panel) and in the reduced Brillouin zone $(-\frac{\pi}{2}, \frac{\pi}{2}]$ (right panel) for $J_x = J_y^{-1} = 1.38$. Note that each subband shows π -periodicity. Here $E(p) = \pm 2\sqrt{4\cos^2(p) + (J_x - J_y)^2}$, where the plus sign refers to the upper branch in the figure, while the minus sign refers to the lower branch.

where M is admissible and the quasi-momenta $\mathbf{p} = (p_1, p_2, \dots, p_M)$ satisfy $e^{iNp_j} = (-1)^{\xi+1}$ for all p_j , form a complete set of mutually orthogonal, normalized eigenstates of the Hamiltonian (18), (20). When rewritten in terms of the quasi-momenta $\{p_j\}$ the energy takes the form

$$\tilde{E}(\mathbf{p}) = \sum_{j=1}^M \pm 2\sqrt{4\cos^2 p_j + (J_x - J_y)^2}, \quad (26)$$

where $+$ holds for $p_j \in (-\pi/2, \pi/2]$ and $-$ for $p_j \in (\pi/2, 3\pi/2]$.

Remark. At the discontinuous points $p = \frac{\pi}{2}, \frac{3\pi}{2}$, the function φ takes the specific values $\varphi(\frac{\pi}{2}) = \varphi(\frac{3\pi}{2}) = \frac{\pi}{4}$.

Remark. Corollary 1 and Theorem 2 are strikingly similar, e.g., the Bethe Ansatz equations for the different sets $\{p_j\}$ are of the same form. As $J_{x,y} \rightarrow 1$ we have $\tilde{\mathcal{A}}_n(p_j) \rightarrow e^{inp_j}$ (for most cases), so the XY eigenvectors reduce to the XX eigenvectors. More details are shown in App. H.

The dispersion relation of our elementary excitations, shown in the left panel of Fig. 3, does not look like that of a single particle. It resembles the dispersion relation of phonons in a harmonic chain in which every second mass has been altered, implying that the size of the unit cell is doubled, while the size of the Brillouin zone is reduced to half of its value. A band gap then opens in the reduced zone scheme and the dispersion is split in an acoustic and an optical branch, representing two different species of phonons, optical and acoustic.

In our case a reduction of the energy-momentum dispersion for all momenta in the interval $(-\pi, +\pi]$ to two subbands in $(-\pi/2, +\pi/2]$ is fully consistent with the chiral Bethe Ansatz solution: the momentum p with values in $(-\pi/2, +\pi/2]$ or $(+\pi/2, +3\pi/2]$ is well-defined, but only $2p$ has a physical meaning. The logarithmic form of the Bethe equations reads for $\xi = 0$ resp. $\xi = 1$

$$p_l = 2n_l \frac{\pi}{N} \mod 2\pi, \quad \text{resp.} \quad p_l = (2n_l - 1) \frac{\pi}{N} \mod 2\pi \quad \text{for } n_l \in \mathbb{Z}, \quad l = 1, \dots, M. \quad (27)$$

Since N is even, p_l and $p_l + \pi$ belong to the same sector (the same value of ξ). This establishes a one-to-one correspondence between the quasi-momenta p_l and $p_l + \pi$ ($-\pi/2 < p_l \leq \pi/2$). The corresponding wave functions are related by

$$\tilde{\mathcal{A}}_n(p_l + \pi) = e^{i[n(p_l + \pi) - \epsilon_n \varphi(p_l + \pi)]} = (-1)^n e^{i[np_l - \epsilon_n \varphi(p_l)]} = (-1)^n \tilde{\mathcal{A}}_n(p_l), \quad -\pi/2 < p_l \leq \pi/2, \quad (28)$$

in full accord with (D17). We further recall that p_l and $p_l + \pi$ yield energies with opposite signs. This means that the particle content of any state can be characterized by two numbers, a momentum $p_l \in (-\frac{\pi}{2}, \frac{\pi}{2}]$ and a “charge” $c_l \in \{-1, 1\}$. The wave functions are

$$\tilde{\mathcal{A}}_n(p_l, c_l) = c_l^n e^{i[np_l - \epsilon_n \varphi(p_l)]}, \quad (29)$$

and the corresponding energies

$$E = 2 \sum_{l=1}^M c_l \sqrt{4 \cos^2 p_l + (J_x - J_y)^2}. \quad (30)$$

Note that this interpretation is well compatible with the fact that the basis states and the vacuum we are building on are invariant under a translation by *two* lattice sites. Since excitations of the Hamiltonian consist of pairs of kinks, their momentum still ranges from $-\pi$ to π . Our kinks are very much like the spinons occurring in the massive XXZ chain in the thermodynamic limit [12]. They can only be created in pairs, the momentum of a single spinon ranges from $-\frac{\pi}{2}$ to $\frac{\pi}{2}$, and they live over a pair of degenerate vacua given by two appropriately deformed Néel states. In our case the occurrence of such excitations is not restricted to the thermodynamic limit. The kinks do exist as bare particles on finite chains, which we find quite interesting.

IV. XY CHIRAL EIGENFUNCTIONS: OBSERVABLES

In the XY case we are as well able to calculate some simple expectation values in chiral eigenstates, which again can be presented in terms of sums of functions of quasimomenta p_j . In Tab. II we compare some observables and conserved quantities for the XX and XY model. A crucial difference between the two models consists in the fact that S^z is not conserved in the XY model. As a consequence, j_l as defined in (14) cannot be interpreted as magnetic current density, but is just a specific two-point operator. Proofs of the statements in the right column of Tab. II are given in Apps. E and F. When one of the periods of the theta functions $\tau \rightarrow +i\infty$, the XY model reduces to the XX model with $J_{x,y} \rightarrow 1$.

Operator of an observable/conserved quantity \hat{A}	XX model expectation $\langle \hat{A} \rangle_{\mathbf{p}}$	XY model expectation $\langle \hat{A} \rangle_{\mathbf{p}}$
transversal magnetization	0	0
energy	$4 \sum_{j=1}^M \cos p_j$	$4 \sum_{j=1}^M \pm \sqrt{\cos^2 p_j + \left(\frac{J_x - J_y}{2}\right)^2}$
“double” momentum $(-i \ln T^2)$	$2 \sum_{j=1}^M p_j + (M + \xi)\pi$	$2 \sum_{j=1}^M p_j + (M + \xi)\pi$
σ_n^z	$\frac{2}{N} \sum_{j=1}^M \sin p_j$	$\frac{J_y^{\epsilon_n}}{N} \sum_{j=1}^M \pm \sin(2p_j) / \sqrt{\cos^2 p_j + \left(\frac{J_x - J_y}{2}\right)^2}$
winding number V	$\frac{1}{4}(N - 2M)$	$\frac{1}{4}(N - 2M)$
$\sigma_l^x \sigma_{l+1}^y - \sigma_l^y \sigma_{l+1}^x$	$1 - \frac{4}{N} \sum_{j=1}^M \sin^2 p_j$	$1 - \frac{4}{N} \sum_{j=1}^M \sin^2 p_j$

TABLE II. Comparison of observables and conserved quantities for chiral XX and XY eigenstates. Here the sign $+$ holds for $p_j \in (-\pi/2, \pi/2]$ and $-$ for $p_j \in (\pi/2, 3\pi/2]$.

V. DISCUSSION

We have constructed a chiral eigenbasis for the XY quantum spin chain, i.e., an orthonormal basis of eigenstates of the XY Hamiltonian that are classified according to their winding number. In the limit of isotropic exchange in the xy -plane we recover the chiral eigenbasis previously constructed [19] for the XX chain. Our solution does not, at any stage, rely on a mapping to non-interacting Fermions. It rather is of Bethe Ansatz type and is a limit of an alternative Bethe Ansatz solution of the more general XYZ quantum spin chain, recently obtained by three of the authors in [30].

We like to interpret the Bethe eigenstates constructed in [30] and reviewed in App. C1 as a chiral eigenbasis for the XYZ model. What is missing so far to complete this interpretation is the construction of an appropriate winding number operator, which remains as a challenge for future work. The very fact that such an alternative Bethe Ansatz exists is of some interest in view the difficulties that seem to persist in attempts (see e.g. [16, 23]) to use the previous Bethe Ansatz solutions [9, 25] for the calculation of matrix elements of local operators between eigenstates. In fact, even the calculation of the norm of the Bethe eigenstates has remained a problem, even in the XY limit [16]. This problem seems absent in the chiral Bethe Ansatz advocated here (cf. App. C3). It would therefore be interesting to lift our work to an algebraic form of the Bethe Ansatz for the XY chain and further on to the more general XYZ chain. This would be an important step towards extending the algebraic Bethe Ansatz approach to the calculation of correlation functions, that was successful for the XXZ chain [10, 13, 14], to the XYZ case.

In Ref. [19] we have seen, in the special case of the XX chain, that overlaps needed for the calculation of certain transverse correlation functions take a simpler form in the chiral eigenbasis than in the S^z eigenbasis. This allowed us to obtain an exact and analytic expression for the time evolution of a one-point function that measures the experimentally realized decay of spin helices [11]. In the present work we have continued our comparison of the description of observables in the chiral eigenbasis and in the S^z eigenbasis, mostly by calculating simple one-point and neighbor two-point correlations in eigenstates of the respective basis.

The chiral Bethe Ansatz for the XY chain offered an interesting physical picture. The excitations that make up the chiral eigenbasis can be interpreted as scattering states of kinks and anti-kinks, topological excitations that can only be created in pairs (two kinks, two anti-kinks, or a kink and an anti-kink). Each individual kink or anti-kink changes the winding number by $\pm\frac{1}{2}$, each pair by 0 or 1. The momenta of the individual kinks and anti-kinks take values in a reduced Brillouin zone $(-\frac{\pi}{2}, \frac{\pi}{2}]$. The kinks and anti-kinks each carry a charge +1 or -1. Depending on this value, their energy is positive or negative. This is in analogy with the spinons in the XXZ chain [12] (for a recent extensive discussion cf. [20, 21]) in its massive antiferromagnetic regime which are generated over two degenerate Néel states of the infinite chain. By way of contrast, our kinks exist on finite chains.

Being an orthonormal basis with factorized structure, the chiral basis should be also well suited for numerical calculations. It can be implemented with usual binary code registers in order to diagonalize any Hamiltonian, which need not be integrable or even a one-dimensional. The chiral basis should perform particularly well, when dealing with problems where topology plays a role, e.g. when the initial quantum state has a helical structure. In this case, as argued in [15], the topological structure gets protected against perturbations like strong local noise, a phenomenon called helical protection by the authors of [15]. The helical protection entails that the temporal dynamics involving transitions between chiral sectors with different winding numbers should be slower than the dynamics within a chiral sector (i.e. not involving transitions between states of different winding number), at least for small times. For a future clarification further studies would be necessary, which is, however, beyond the scope of the present communication.

ACKNOWLEDGMENT

X. Z. acknowledges financial support from the National Natural Science Foundation of China (No. 12204519). F. G. would like to thank J.-M. Maillet for a stimulating discussion. F. G. and A. K. acknowledge financial support by Deutsche Forschungsgemeinschaft through FOR 2316. A. K. also gratefully acknowledges support through a fellowship from the Chinese Academy of Sciences and the Innovation Academy for Precision Measurement Science and Technology, Wuhan. V. P. acknowledges support by Deutsche Forschungsgemeinschaft through DFG project KL 645/20-2 and by an ERC Advanced grant No. 101096208 – QUEST.

-
- [1] R. J. Baxter, *Generalized ferroelectric model on a square lattice*, Stud. Appl. Math. **50** (1971), 51–69.
 - [2] ———, *Eight-vertex model in lattice statistics and one-dimensional anisotropic Heisenberg chain. I. Some fundamental eigenvectors*, Ann. Phys. (N.Y.) **76** (1973), 1–24.
 - [3] ———, *Eight-vertex model in lattice statistics and one-dimensional anisotropic Heisenberg chain. II. Equivalence to a generalized ice-type lattice model*, Ann. Phys. (N.Y.) **76** (1973), 25–47.
 - [4] ———, *Eight-vertex model in lattice statistics and one-dimensional anisotropic Heisenberg chain. III. Eigenvectors of the transfer matrix and Hamiltonian*, Ann. Phys. (N.Y.) **76** (1973), 48–71.
 - [5] Rodney J Baxter, *Exactly Solved Models in Statistical Mechanics*, Academic Press, 1982.
 - [6] J. Cao, W.-L. Yang, K. Shi, and Y. Wang, *Off-diagonal Bethe ansatz solutions of the anisotropic spin-1/2 chains with arbitrary boundary fields*, Nucl. Phys. B **877** (2013), 152–175.
 - [7] F. Colomo, A. G. Izergin, V. E. Korepin, and V. Tognetti, *Temperature correlation functions in the XX0 Heisenberg chain. I*, Theor. Math. Phys. **94** (1993), 11–38.
 - [8] I. Dimitrova, S. Flannigan, Y. K. Lee, H. Lin, J. Amato-Grill, N. Jepsen, I. Cebaite, A. J. Daley, and W. Ketterle, *Many-body spin rotation by adiabatic passage in spin-1/2 XXZ chains of ultracold atoms*, Quantum Sci. Technol. **8** (2023), 035018.
 - [9] G. Felder and A. Varchenko, *Algebraic Bethe ansatz for the elliptic quantum group $E_{\tau,\eta}(sl_2)$* , Comm. Math. Phys. **480** (1996), 485–503.
 - [10] F. Göhmann, A. Klümper, and A. Seel, *Integral representations for correlation functions of the XXZ chain at finite temperature*, J. Phys. A **37** (2004), 7625–7652.
 - [11] P. N. Jepsen, Y. K. Lee, H. Lin, I. Dimitrova, Y. Margalit, W. W. Ho, and W. Ketterle, *Long-lived phantom helix states in Heisenberg quantum magnets*, Nature Physics **18** (2022), 899–904.
 - [12] M. Jimbo and T. Miwa, *Algebraic analysis of solvable lattice models*, American Mathematical Society, 1995.

- [13] N. Kitanine, J. M. Maillet, and V. Terras, *Form factors of the XXZ Heisenberg spin- $\frac{1}{2}$ finite chain*, Nucl. Phys. B **554** (1999), 647–678.
- [14] ———, *Correlation functions of the XXZ Heisenberg spin- $\frac{1}{2}$ chain in a magnetic field*, Nucl. Phys. B **567** (2000), 554–582.
- [15] S. Kühn, F. Gerken, L. Funcke, T. Hartung, P. Stornati, K. Jansen, and T. Posske, *Quantum spin helices more stable than the ground state: Onset of helical protection*, Phys. Rev. B **107** (2023), 214422.
- [16] G. Kulkarni and N. A. Slavnov, *Scalar products of Bethe vectors in the generalized algebraic Bethe ansatz*, Theor. Math. Phys. **217** (2023), 1574–1594.
- [17] E. H. Lieb, T. Schultz, and D. Mattis, *Two soluble models of an antiferromagnetic chain*, Ann. Phys. (N.Y.) **16** (1961), 407–466.
- [18] D. Mumford, *Tata lectures on theta i*, Birkhäuser Verlag, Basel, 1982, Progress in Math. 28.
- [19] V. Popkov, X. Zhang, F. Göhmann, and A. Klümper, *Chiral basis for qubits and spin-helix decay*, Phys. Rev. Lett. **132** (2024), 220404.
- [20] S. B. Rutkevich, *Spinon confinement in the gapped antiferromagnetic XXZ spin- $\frac{1}{2}$ chain*, Phys. Rev. B **106** (2022), 134405.
- [21] ———, *Confinement of spinons in the XXZ spin- $\frac{1}{2}$ chain in presence of a transverse magnetic field*, Phys. Rev. B **109** (2024), 014411.
- [22] E. K. Sklyanin, L. A. Takhtadzhyan, and L. D. Faddeev, *Quantum inverse problem method. I.*, Theor. Math. Phys. **40** (1979), 688–706.
- [23] N. Slavnov, A. Zabrodin, and A. Zotov, *Scalar products of Bethe vectors in the 8-vertex model*, J. High Energy Phys. **2020** (2020), 123.
- [24] B. Sutherland, *Exact solution of a two-dimensional model for hydrogen-bonded crystals*, Phys. Rev. Lett. **19** (1967), 103–104.
- [25] L. A. Takhtajan and L. D. Faddeev, *The quantum method of the inverse problem and the Heisenberg XYZ model*, Usp. Mat. Nauk **34** (1979), no. 5, 13.
- [26] A. Venegas-Gomez, A. S. Buyskikh, J. Schachenmayer, W. Ketterle, and A. J. Daley, *Dynamics of rotated spin states and magnetic ordering with two-component bosonic atoms in optical lattices*, Phys. Rev. A **102** (2020), 023321.
- [27] A. Venegas-Gomez, J. Schachenmayer, A. S. Buyskikh, W. Ketterle, M. L. Chiofalo, and A. J. Daley, *Adiabatic preparation of entangled, magnetically ordered states with cold bosons in optical lattices*, Quantum Sci. Technol. **5** (2020), 045013.
- [28] Y. Wang, W.-L. Yang, J. Cao, and K. Shi, *Off-Diagonal Bethe Ansatz for Exactly Solvable Models*, Springer, 2016.
- [29] E. T. Whittaker and G. N. Watson, *A Course of Modern Analysis*, Cambridge University Press, 1950.
- [30] X. Zhang, A. Klümper, and V. Popkov, *Pedestrian’s way to Baxter’s Bethe ansatz for the periodic XYZ chain*, Phys. Rev. B **109** (2024), 115411.

Appendix A: Theta functions

Following Ref. [29], but rescaling the arguments by π we define the four Jacobi theta functions

$$\begin{aligned}
 \theta_1(u, q) &= 2 \sum_{n=0}^{\infty} (-1)^n q^{(n+\frac{1}{2})^2} \sin[(2n+1)\pi u], \\
 \theta_2(u, q) &= 2 \sum_{n=0}^{\infty} q^{(n+\frac{1}{2})^2} \cos[(2n+1)\pi u], \\
 \theta_3(u, q) &= 1 + 2 \sum_{n=1}^{\infty} q^{n^2} \cos(2n\pi u), \\
 \theta_4(u, q) &= 1 + 2 \sum_{n=1}^{\infty} (-1)^n q^{n^2} \cos(2n\pi u).
 \end{aligned} \tag{A1}$$

Appendix B: Commutativity of H_{XY} and V

Here we show that the XY Hamiltonian commutes with V defined in (7). Let us split the XY Hamiltonian into two parts, the X -part and the Y -part,

$$H_{XY} = J_x \sum_{n=1}^N \sigma_n^x \sigma_{n+1}^x + J_y \sum_{n=1}^N \sigma_n^y \sigma_{n+1}^y, \tag{B1}$$

where N is even, and prove the commutativity of each part with V individually.

For the X -part we have

$$\begin{aligned}
4 \left[\sum_{n=1}^N \sigma_n^x \sigma_{n+1}^x, V \right] &= \left[\sum_{n=1}^N \sigma_n^x \sigma_{n+1}^x, \sum_{l=1}^{N/2} (\sigma_{2l-1}^x \sigma_{2l}^y - \sigma_{2l}^y \sigma_{2l+1}^x) \right] \\
&= \left[\sum_{n=1}^{N/2} (\sigma_{2n-1}^x \sigma_{2n}^x + \sigma_{2n}^x \sigma_{2n+1}^x), \sum_{l=1}^{N/2} (\sigma_{2l-1}^x \sigma_{2l}^y - \sigma_{2l}^y \sigma_{2l+1}^x) \right] \\
&= (2i - 2i) \sum_{n=1}^{N/2} \sigma_{2n}^z + (2i - 2i) \sum_{n=1}^{N/2} \sigma_{2n-1}^x \sigma_{2n}^z \sigma_{2n+1}^x = 0.
\end{aligned} \tag{B2}$$

Analogously, we check the commutativity of the Y -part in (B1) with V . Thus, we obtain

$$[H_{XY}, V] = 0, \tag{B3}$$

and, consequently, the XY-model can be diagonalized within blocks with a fixed (and admissible) number of kinks M .

Appendix C: Chiral Bethe vectors of the XY model

1. Chiral coordinate Bethe Ansatz for the periodic XYZ chain

Let us first consider the general periodic XYZ chain

$$H_{XYZ} = \sum_{n=1}^N (J_x \sigma_n^x \sigma_{n+1}^x + J_y \sigma_n^y \sigma_{n+1}^y + J_z \sigma_n^z \sigma_{n+1}^z). \tag{C1}$$

The exchange coefficients $\{J_x, J_y, J_z\}$ are parameterized by the crossing parameter η as [5, 6, 28]

$$J_x = \frac{\theta_4(\eta)}{\theta_4(0)}, \quad J_y = \frac{\theta_3(\eta)}{\theta_3(0)}, \quad J_z = \frac{\theta_2(\eta)}{\theta_2(0)}. \tag{C2}$$

In Ref. [30], the periodic XYZ chains with η satisfying the following root-of-unity condition has been studied

$$\begin{aligned}
(N - 2M)\eta &= 2L\tau + 2K, \quad 0 \leq M \leq N, \quad L, K \in \mathbb{Z}, \\
s\eta &= 2L_0\tau + 2K_0, \quad s \in \mathbb{N}^+, \quad L_0, K_0 \in \mathbb{Z},
\end{aligned} \tag{C3}$$

where s is the smallest positive integer satisfying Eq. (C3).

Define the following local state

$$\phi(v) = \begin{pmatrix} \theta_1(v, q^2) \\ \theta_4(v, q^2) \end{pmatrix}, \quad v \in \mathbb{C}, \tag{C4}$$

Then we can construct a set of factorized states [30]

$$\begin{aligned}
&|d; n_1, n_2, \dots, n_M\rangle_{xyz} \\
&= \bigotimes_{l_1=1}^{n_1} \phi(v_{2d+l_1}) \bigotimes_{l_2=n_1+1}^{n_2} \phi(v_{2d+l_2-2}) \cdots \\
&\cdots \bigotimes_{l_M=n_{M-1}+1}^{n_M} \phi(v_{2d+l_M-2M+2}) \bigotimes_{l_{M+1}=n_M+1}^N \phi(v_{2d+l_{M+1}-2M}), \\
&1 \leq n_1 < n_2 < \dots < n_M \leq N.
\end{aligned} \tag{C5}$$

where $v_m = v_1 + (m-1)\eta$. Under the root-of-unity condition (C3), the vectors

$$|d; n_1, n_2, \dots, n_M\rangle_{xyz}, \quad d = 0, 1, \dots, s-1,$$

$$1 \leq n_1 < n_2 < \dots < n_M \leq N, \quad (\text{C6})$$

form an invariant subspace of the Hilbert space. The eigenstates of H_{XYZ} thus can be expanded as

$$|\Psi_M(\mathbf{u})\rangle_{xyz} = \sum_{d=0}^{s-1} \sum_{\mathbf{n}} F_{M,d,\mathbf{n}}(\mathbf{u}) |d; n_1, \dots, n_M\rangle_{xyz}, \quad (\text{C7})$$

where $\mathbf{n} = \{n_1, \dots, n_M\}$ with $1 \leq n_1 < n_2 < \dots < n_M \leq N$, which applies to the following sections in the appendix. The expansion coefficients $\{F_{M,d,\mathbf{n}}(\mathbf{u})\}$ are given by the chiral coordinate Bethe Ansatz method [30]. In this paper we only consider the case where η is real ($L = L_0 = 0$ in Eq. (C3)), and $\{F_{M,d,\mathbf{n}}(\mathbf{u})\}$ now reads

$$F_{M,d,\mathbf{n}}(\mathbf{u}) = e^{-d\omega} \sum_{x_1, \dots, x_M} C_{x_1, \dots, x_M} \prod_{l=1}^M U_{2d-2l+n_l+2}^{(n_l)}(u_{x_l}), \quad (\text{C8})$$

where $U_m^{(n)}(v)$ is defined by

$$U_m^{(n)}(v) = \left[\frac{\theta_1(v + \frac{\eta}{2})}{\theta_1(v - \frac{\eta}{2})} \right]^n \frac{\theta_2(v - v_m + \frac{\eta}{2})}{\theta_2(v_{m-1})\theta_2(v_m)}, \quad (\text{C9})$$

and $\{x_1, \dots, x_M\}$ is a permutation of $\{1, \dots, M\}$. The coefficients $\{C_{x_1, \dots, x_M}\}$ in terms of Bethe roots $\{u_1, \dots, u_M\}$ satisfy

$$\frac{C_{\dots, x_{n+1}, x_n, \dots}}{C_{\dots, x_n, x_{n+1}, \dots}} = \frac{\theta_1(u_{x_n} - u_{x_{n+1}} - \eta)}{\theta_1(u_{x_n} - u_{x_{n+1}} + \eta)}. \quad (\text{C10})$$

The Bethe roots $\{u_1, \dots, u_M\}$ and the parameter ω satisfy the following Bethe Ansatz equations

$$e^{\omega} \left[\frac{\theta_1(u_j + \frac{\eta}{2})}{\theta_1(u_j - \frac{\eta}{2})} \right]^N \prod_{l \neq j}^M \frac{\theta_1(u_j - u_l - \eta)}{\theta_1(u_j - u_l + \eta)} = 1, \quad e^{s\omega} = 1, \quad j = 1, 2, \dots, M. \quad (\text{C11})$$

The energy in terms of the Bethe roots reads

$$E_{xyz}(\mathbf{u}) = 2 \frac{\theta_1(\eta)}{\theta_1'(0)} \sum_{j=1}^M \left[\frac{\theta_1'(u_j - \frac{\eta}{2})}{\theta_1(u_j - \frac{\eta}{2})} - \frac{\theta_1'(u_j + \frac{\eta}{2})}{\theta_1(u_j + \frac{\eta}{2})} \right] + N \frac{\theta_1'(\eta)}{\theta_1'(0)}. \quad (\text{C12})$$

2. Reduction from the XYZ Model to the XY Model

When $\eta = \frac{1}{2}$, the XYZ chain (C1) reduces to the XY chain as follows

$$\{J_x, J_y, J_z\} = \left\{ \frac{\theta_3(0)}{\theta_4(0)}, \frac{\theta_4(0)}{\theta_3(0)}, 0 \right\}. \quad (\text{C13})$$

Consider a periodic XY chain with an even number of sites. Then we can get the value of M and s in Eq. (C3),

$$s = 2, \quad M = 0, 2, \dots, N, \quad \text{for } N = 4m, \quad m \in \mathbb{N}^+, \quad (\text{C14})$$

$$s = 2, \quad M = 1, 3, \dots, N-1, \quad \text{for } N = 4m+2, \quad m \in \mathbb{N}. \quad (\text{C15})$$

Therefore, we can directly obtain the chiral Bethe state of the XY chain from the results for the XYZ chain. By letting $v_1 = \frac{1+\tau}{2}$ and eliminating an overall factor in (C6) and (C7), we finally arrive at the Bethe state given by Eq. (21).

Remark. When $\eta = \frac{1}{2}$, we see that $J_x/J_y > 0$. By letting $\eta = -\frac{1}{2} - \tau$, the XYZ chain (C1) reduces to another XY model with

$$\{J_x, J_y, J_z\} = e^{-i\pi\tau} \left\{ \frac{\theta_3(0)}{\theta_4(0)}, -\frac{\theta_4(0)}{\theta_3(0)}, 0 \right\}. \quad (\text{C16})$$

3. Normalization and orthogonality of Bethe vectors

Since the $|\Psi_M(\mathbf{u})\rangle$ are simultaneous eigenvectors of H_{XY} and V , the scalar products $\langle\Psi_M(\mathbf{u})|\Psi_{M'}(\mathbf{u}')\rangle$ with $M \neq M'$ all vanish.

Using the orthonormality of the chiral basis states

$$\langle\iota; \mathbf{m}|\kappa; \mathbf{n}\rangle = \delta_{\iota,\kappa}\delta_{\mathbf{m},\mathbf{n}} \quad (\text{C17})$$

and the properties of the determinant, we first of all see that

$$\begin{aligned} \langle\Psi_M(\mathbf{u})|\Psi_M(\mathbf{u}')\rangle &= \sum_{\substack{1 \leq m_1 < \dots < m_M \leq N \\ 1 \leq n_1 < \dots < n_M \leq N}} \sum_{\iota, \kappa = \pm 1} \chi_{\mathbf{m}}(\mathbf{u})^* \chi_{\mathbf{n}}(\mathbf{u}') \iota^\xi \kappa^{-\xi'} \langle\iota; \mathbf{m}|\kappa; \mathbf{n}\rangle \\ &= \sum_{1 \leq n_1 < \dots < n_M \leq N} \sum_{\kappa = \pm 1} \kappa^{\xi - \xi'} \chi_{\mathbf{n}}(\mathbf{u})^* \chi_{\mathbf{n}}(\mathbf{u}') = 2\delta_{\xi, \xi'} \sum_{1 \leq n_1 < \dots < n_M \leq N} \chi_{\mathbf{n}}(\mathbf{u})^* \chi_{\mathbf{n}}(\mathbf{u}') \\ &= \frac{\delta_{\xi, \xi'}}{M! N^M} \sum_{\mathbf{n} \in \{1, \dots, N\}^M} \det_M \{\mathcal{A}_{n_j}(u_k)^*\} \det_M \{\mathcal{A}_{n_j}(u'_k)\} \\ &= \frac{\delta_{\xi, \xi'}}{M! N^M} \sum_{\mathbf{n} \in \{1, \dots, N\}^M} \sum_{Q \in \mathfrak{S}^M} \text{sign}(Q) \mathcal{A}_{n_{Q^1}}(u_1)^* \dots \mathcal{A}_{n_{Q^M}}(u_M)^* \det_M \{\mathcal{A}_{n_j}(u'_k)\} \\ &= \frac{\delta_{\xi, \xi'}}{M! N^M} \sum_{\mathbf{n} \in \{1, \dots, N\}^M} \sum_{Q \in \mathfrak{S}^M} \mathcal{A}_{n_{Q^1}}(u_1)^* \dots \mathcal{A}_{n_{Q^M}}(u_M)^* \det_M \{\mathcal{A}_{n_{Q^j}}(u'_k)\} \\ &= \frac{\delta_{\xi, \xi'}}{M! N^M} \sum_{Q \in \mathfrak{S}^M} \det_M \left\{ \sum_{n=1}^N \mathcal{A}_n(u_j)^* \mathcal{A}_n(u'_k) \right\} = \frac{\delta_{\xi, \xi'}}{N^M} \det_M \left\{ \sum_{n=1}^N \mathcal{A}_n(u_j)^* \mathcal{A}_n(u'_k) \right\}. \end{aligned} \quad (\text{C18})$$

Here we have used (C17) in the second equation, the fact that $\xi, \xi' \in \{0, 1\}$ in the third equation, the definition (21) of $\chi_{\mathbf{n}}(\mathbf{u})$ in the fourth equation, the definition of the determinant as a sum of permutations in the fifth equation, the antisymmetry of the determinant in the sixth equation, the multi-linearity of the determinant in the seventh equation, and the fact that the number of elements in the symmetric group is $M!$ in the last equation.

It remains to evaluate the sum inside the determinant on the right hand side of (C18). For this purpose we notice that

$$\sum_{n=1}^N \mathcal{A}_n(u_j)^* \mathcal{A}_n(u'_k) = \sum_{n=1}^N \tilde{\mathcal{A}}_n(p_j)^* \tilde{\mathcal{A}}_n(p'_k) = e^{i(\varphi(p_j) - \varphi(p'_k))} \sum_{n=1}^{N/2} e^{i2n(p'_k - p_j)} + e^{i(\varphi(p'_k) - \varphi(p_j))} \sum_{n=1}^{N/2} e^{i(2n-1)(p'_k - p_j)}, \quad (\text{C19})$$

where $p_j = p(u_j)$, $p'_k = p(u'_k)$ and where we have used (25). As a direct consequence of the geometric sum formula we have the identities

$$\sum_{n=1}^{N/2} x^{2n} = \begin{cases} x^2 \frac{1-x^N}{1-x^2} & \text{if } x^2 \neq 1 \\ \frac{N}{2} & \text{if } x^2 = 1 \end{cases}, \quad \sum_{n=1}^{N/2} x^{2n-1} = \begin{cases} x \frac{1-x^N}{1-x^2} & \text{if } x^2 \neq 1 \\ x \frac{N}{2} & \text{if } x^2 = 1 \end{cases}. \quad (\text{C20})$$

We shall use these identities for $x = e^{i(p'_k - p_j)}$. The Bethe Ansatz equations in Corollary 1 for $\xi = \xi'$ then imply that $x^N = 1$, and

$$\sum_{n=1}^N \tilde{\mathcal{A}}_n(p_j)^* \tilde{\mathcal{A}}_n(p'_k) = 0, \quad (\text{C21})$$

if $x^2 \neq 1$.

If $x = -1$, then $p'_k - p_j = \pi \pmod{2\pi}$; if $x = 1$, then $p'_k - p_j = 0 \pmod{2\pi}$. It follows in both cases from the π -periodicity of the function φ that $\varphi(p'_k) = \varphi(p_j)$. Thus,

$$\sum_{n=1}^N \tilde{\mathcal{A}}_n(p_j)^* \tilde{\mathcal{A}}_n(p'_k) = (1+x) \frac{N}{2}, \quad (\text{C22})$$

if $x^2 = 1$.

Using now (C19), (C21) and (C22) in (C18) we have proved the orthonormality condition $\langle\Psi_M(\mathbf{u})|\Psi_M(\mathbf{u}')\rangle = \delta_{\mathbf{u}, \mathbf{u}'}$. Then a simple counting argument as employed in the XX case in [19] implies that the chiral eigenstates form a basis.

Appendix D: Quasi-momentum representation of Bethe states and dispersion relation for the XY model

In this appendix we want to define the quasimomentum $p(u)$ in terms of a suitable, elementary elliptic function

$$r(u) := \frac{\theta_1(u + \frac{1}{4})}{\theta_1(u - \frac{1}{4})} \equiv e^{ip(u)}, \quad (D1)$$

and to express all other elliptic functions, especially the ratio of θ_3 functions in (21) and the energy (23)

$$R(u) := \frac{\theta_3(u + \frac{1}{4})}{\theta_3(u - \frac{1}{4})}, \quad \mathcal{E}(u) := 2 \frac{\theta_2(0)}{\theta_1'(0)} \left[\frac{\theta_1'(u - \frac{1}{4})}{\theta_1(u - \frac{1}{4})} - \frac{\theta_1'(u + \frac{1}{4})}{\theta_1(u + \frac{1}{4})} \right], \quad (D2)$$

in explicit terms of $p(u)$ thus avoiding the use of elliptic functions in “practical calculations”.

We use several properties of the function $r(u)$

$$r(u + \frac{1}{2}) = -\frac{1}{r(u)}, \quad r(u + \tau) = -r(u), \quad r(-u) = \frac{1}{r(u)}, \quad r(u + \frac{1}{2} + \tau) = \frac{1}{r(u)}, \quad (D3)$$

which follow more or less directly from the definition and elementary properties of the θ -functions. We have several special values of $r(u)$

$$r(0) = -1, \quad r(\pm \frac{\tau}{2}) = \mp i, \quad r(\tau) = 1, \quad (D4)$$

$$\pm r(\frac{1}{4} \pm \frac{\tau}{2}) = -\frac{i}{J_y}, \quad \pm r(-\frac{1}{4} \pm \frac{\tau}{2}) = -iJ_y, \quad r'(\pm \frac{1}{4} \pm \frac{\tau}{2}) = 0, \quad (D5)$$

where the identities in the second line follow from the symmetry $r(u + \frac{1}{2} + \tau) = r(-u)$ (see (D3)) and

$$J_y = \frac{1}{J_x} = \frac{\theta_4(0)}{\theta_3(0)} = -i \frac{\theta_1(\frac{\tau}{2})}{\theta_1(\frac{1}{2} + \frac{\tau}{2})}. \quad (D6)$$

Expression of $R(u)$ in terms of $r(u)$

We have the identity

$$R(u)^2 = \frac{r(u)^2 J_y^2 + 1}{r(u)^2 + J_y^2}, \quad (D7)$$

which is proven by use of Liouville's theorem. We note that both sides are meromorphic functions and doubly periodic with periods $1, \tau$. The two sides have same poles and zeros and evaluate to 1 for argument $u = 0$. In detail: the poles of $r(u)$ on the RHS cancel in the ratio. The only poles of the RHS are the zeros of the denominator. The only pole of the LHS in the period rectangle (width 1, height τ) is $-\frac{1}{4} - \frac{\tau}{2}$ and of degree 2. This point is a zero of the denominator of the RHS, and it is a zero of 2nd order due to the vanishing of the derivative of $r(u)$ at this point (the second derivative can not be zero). In a similar way we see that $\frac{1}{4} - \frac{\tau}{2}$ is a zero of second order of LHS and RHS. Special value of LHS and RHS at $u = 0$: use $R(0) = +1$, $r(0) = -1$.

Now we see that $R(u)$ can be calculated from $r(u) = e^{ip}$

$$R(u) = \mp \sqrt{\frac{J_y^2 + 1/r(u)^2}{J_y^2 + r(u)^2}} r(u) \quad \text{for } J_y^2 > 1 \quad \text{and} \quad = \mp \sqrt{\frac{1 + J_y^2 r(u)^2}{1 + J_y^2 / r(u)^2}} \frac{1}{r(u)} \quad \text{for } J_y^2 < 1, \quad (D8)$$

where the sign $- (+)$ holds for $u \in i\mathbb{R}$ ($u \in i\mathbb{R} + 1/2$) and the square root is the standard one with branch cut along $(-\infty, 0]$. (In the main text, e.g. Fig. 3 the second case in (D8) applies.) Note that the argument of the square root lies on the unit circle and never hits -1 . The signs are then fixed by considering the points $u = 0$ and $u = 1/2$ yielding $r(0) = -1$, $R(0) = +1$ and $r(1/2) = R(1/2) = +1$.

The dispersion relation: $\mathcal{E}(u)$ in terms of $r(u)$

We have the identity

$$-\left[\frac{\theta_1'(0)}{\theta_2(0)} \frac{\theta_1(\frac{\tau}{2})}{\theta_1(\frac{1}{2} + \frac{\tau}{2})} \right]^2 \left[r(u)^2 + \frac{1}{J_y^2} \right] \left[\frac{1}{r(u)^2} + \frac{1}{J_y^2} \right] = \left[\frac{\theta_1'(u - \frac{1}{4})}{\theta_1(u - \frac{1}{4})} - \frac{\theta_1'(u + \frac{1}{4})}{\theta_1(u + \frac{1}{4})} \right]^2, \quad (D9)$$

which is proven by using Liouville's theorem. We note that both sides are meromorphic functions and doubly periodic with periods $1, \tau$. For $r(u)$ the shift of u by τ leads to a minus sign, but that drops out on the LHS. The shift by τ in the argument leaves the RHS invariant as the logarithmic derivatives of θ_1 yield the same cancelling additive constant

$$\frac{\theta'_1(u+\tau)}{\theta_1(u+\tau)} = -2\pi i + \frac{\theta'_1(u)}{\theta_1(u)}. \quad (\text{D10})$$

Obviously, both sides have the same two poles per period rectangle, e.g. at $u = \pm 1/4$, each of order 2. Both sides have the same zeros of order 2 at $u = \pm 1/4 + \tau/2$. The zeros deserve more explanations: Inserting in (D10) $u = -\tau/2$ and using that θ_1 is an odd function we get

$$\frac{\theta'_1(\frac{\tau}{2})}{\theta_1(\frac{\tau}{2})} = -2\pi i + \frac{\theta'_1(-\frac{\tau}{2})}{\theta_1(-\frac{\tau}{2})} = -2\pi i - \frac{\theta'_1(\frac{\tau}{2})}{\theta_1(\frac{\tau}{2})}. \quad (\text{D11})$$

Inserting in (D10) $u = 1/2 - \tau/2$ and using that θ_1 is an odd function with period 1 we get

$$\frac{\theta'_1(\frac{1+\tau}{2})}{\theta_1(\frac{1+\tau}{2})} = -2\pi i + \frac{\theta'_1(\frac{1-\tau}{2})}{\theta_1(\frac{1-\tau}{2})} = -2\pi i - \frac{\theta'_1(\frac{1+\tau}{2})}{\theta_1(\frac{1+\tau}{2})}. \quad (\text{D12})$$

So we get

$$\frac{\theta'_1(\frac{\tau}{2})}{\theta_1(\frac{\tau}{2})} = \frac{\theta'_1(\frac{1+\tau}{2})}{\theta_1(\frac{1+\tau}{2})} = -\pi i. \quad (\text{D13})$$

Therefore $u = 1/4 + \tau/2$ is a zero of the RHS of (D9) and clearly of order 2. And the same holds for $u = -1/4 + \tau/2$.

The two points $u = \pm 1/4 + \tau/2$ are clearly also zeros of the LHS and of order 2. This is because the derivative of $r(u)$ at these points is zero (and the second derivative has to be non-zero).

Now we know that the ratio of LHS and RHS has to be constant, which can be obtained from evaluating the leading behaviour at the pole at $u = 1/4$.

Now we obtain the expression for the energy $\mathcal{E}(u)$ by multiplying (D9) with the square of $2\theta_2(0)/\theta'_1(0)$

$$\begin{aligned} \frac{\mathcal{E}^2(u)}{4} &= J_y^2 \left[r(u)^2 + \frac{1}{J_y^2} \right] \left[\frac{1}{r(u)^2} + \frac{1}{J_y^2} \right] = r(u)^2 + \frac{1}{r(u)^2} + J_y^2 + \frac{1}{J_y^2} \\ &= \left[r(u) + \frac{1}{r(u)} \right]^2 + \left[J_y - \frac{1}{J_y} \right]^2 = 4 \cos^2 p(u) + (J_y - J_x)^2, \end{aligned} \quad (\text{D14})$$

from which follows

$$\mathcal{E}(u) = \mp 2 \sqrt{4 \cos^2 p(u) + (J_y - J_x)^2}, \quad (\text{D15})$$

where the sign $- (+)$ holds for $u \in i\mathbb{R}$ ($u \in i\mathbb{R} + 1/2$). The sign is fixed by realizing $\mathcal{E}(0) > 0$ and $\mathcal{E}(u+1/2) = -\mathcal{E}(u)$. Alternatively, with the definition of the invertible momentum function $p(u)$ (see below) we find $-$ holds for $p \in (\pi/2, 3\pi/2]$ and $+$ for $p \in (-\pi/2, \pi/2]$.

Finally we arrive at the following identity

$$i \left[\frac{1}{r(u)R^{\pm 1}(u)} - r(u)R^{\pm 1}(u) \right] = 4J_y^{\pm 1} \frac{\sin[2p(u)]}{\mathcal{E}(u)} =: \mathcal{X}(u, \pm 1), \quad (\text{D16})$$

where we define the right hand side as function \mathcal{X} .

Lines on which $r(u)$ takes unimodular values and $p(u)$ is real

We see directly that $r(u)$ takes values of absolute value 1 on the imaginary axis and on the imaginary axis shifted by $1/2$. From (D4) we see that $r(u)$ runs over the unit circle for $u \in [-\tau, \tau]$ starting at $+1$ for $u = -\tau$, being $+i$ for $u = -\tau/2$, -1 for $u = 0$, $-i$ for $u = \tau/2$ and ending at $+1$ for $u = +\tau$. Similarly the unit circle is surrounded in positive sense for $u \in [\tau, -\tau] + 1/2$, however beginning with -1 at $u = \tau + 1/2$ and then decreasing the imaginary part of u .

In this way all points of the unit circle are visited in the period rectangle (width 1, height 2τ) at least two times. The precise number of such visits has to be 2 as the number of poles is 2. Hence the above described motion of $r(u)$

around the unit circle has to be monotonous. If not, then certain points would be visited at least 3 times which would result in a contradiction. Also we see that only on the imaginary axis and the imaginary axis shifted by $1/2$ values on the unit circle are taken.

The quasimomentum $p(u)$ as invertible function

Each value of the unit circle is taken by the function $r(u)$ at two points in the period rectangle (width 1, height 2τ): this is for some imaginary value u and for the point $-u + 1/2 + \tau$. The inverse map from the unit circle to the period rectangle is obviously not uniquely defined.

On the other hand, we have $r(u) = -r(u + \tau)$ and $R(u) = -R(u + \tau)$. From this and (21) we obtain

$$\mathcal{A}_n(u) R(u)^{1/2} r(u) = r(u)^{2m} \cdot \begin{cases} \mp \sqrt{\frac{1+J_y^2 r(u)^2}{1+J_y^2/r(u)^2}}, & n = 2m, \\ 1, & n = 2m - 1, \end{cases} \quad (\text{D17})$$

where the sign $- (+)$ holds for $u \in i\mathbb{R}$ ($u \in i\mathbb{R} + 1/2$). From (D17) we see that u and $u + \tau$ lead to the same state. This is “consistent” with the property $\mathcal{E}(u) = \mathcal{E}(u + \tau)$. Therefore, we consider u and $u + \tau$ as equivalent. Now we consider solutions u_j to the Bethe equations on $i\mathbb{R}$ reduced to the interval $(-\tau/2, +\tau/2]$, and on $i\mathbb{R} + 1/2$ reduced to $(\tau/2, -\tau/2] + 1/2$. The function $r(u)$ on the first interval parameterizes the semi-circle from $+i$ over -1 to $-i$ (first point excluded). On the second interval it parameterizes the semi-circle from $-i$ over $+1$ to $+i$ (first point excluded). Finally we choose $p(u)$ to take values on the first interval out of $(\pi/2, 3\pi/2]$, and on the second interval out of $(-\pi/2, +\pi/2]$.

From (D17) we find

$$\frac{\mathcal{A}_{2m}(u)}{\mathcal{A}_{2m-1}(u)} = \mp \sqrt{\frac{1+J_y^2 r(u)^2}{1+J_y^2/r(u)^2}} = \mp e^{i[p(u)-2\varphi(p)]}, \quad \text{where} \quad \tan(2\varphi) = \frac{J_x - J_y}{J_x + J_y} \tan p. \quad (\text{D18})$$

Appendix E: Magnetization of the XY model

For the one-point correlation $\langle \sigma_n^{x,y,z} \rangle$, we observe that

$$\langle \Psi_M(\mathbf{u}) | \sigma_n^{x,y} | \Psi_M(\mathbf{u}) \rangle = 0, \quad (\text{E1})$$

$$\langle \Psi_M(\mathbf{u}) | \sigma_n^z | \Psi_M(\mathbf{u}) \rangle = \frac{1}{N} \sum_{l=1}^M \mathcal{X}(u_l, (-1)^n), \quad (\text{E2})$$

where $\mathcal{X}(u, \pm 1)$ was defined in (D16).

Proof. The state $|\Psi_M(\mathbf{u})\rangle$ can be rewritten as

$$|\Psi_M(\mathbf{u})\rangle = O \sum_{\mathbf{n}} \chi_{\mathbf{n}}(\mathbf{u}) |1; \mathbf{n}\rangle, \quad (\text{E3})$$

where

$$O = \mathbb{I} + (-1)^\xi \sigma_1^z \sigma_2^z \cdots \sigma_N^z, \quad \xi = \pm 1. \quad (\text{E4})$$

With the help of the operator O , we can easily prove that

$$O^\dagger \sigma_n^x O = O^\dagger \sigma_n^y O = 0. \quad (\text{E5})$$

Therefore, one readily gets

$$\langle \Psi_M(\mathbf{u}) | \sigma_n^x | \Psi_M(\mathbf{u}) \rangle = \langle \Psi_M(\mathbf{u}) | \sigma_n^y | \Psi_M(\mathbf{u}) \rangle = 0. \quad (\text{E6})$$

From Eq. (E5), one can also prove that

$$\left\langle \sigma_{j_1}^{\alpha_1} \sigma_{j_2}^{\alpha_2} \cdots \sigma_{j_{2k+1}}^{\alpha_{2k+1}} \right\rangle = 0, \quad \alpha_{j_1}, \dots, \alpha_{j_{2k+1}} = x, y. \quad (\text{E7})$$

Define an operator T , which shifts the lattice to the left by one site. One can prove

$$\begin{aligned} T^2 |\kappa; n\rangle &= (-i)^2 |-\kappa; n-2\rangle, \quad n \geq 3, \\ T^2 |\kappa; n\rangle &= (-i)^{N-2} |\kappa; n-2+N\rangle, \quad n = 1, 2, \end{aligned} \quad (\text{E8})$$

$$\begin{aligned} T^2 |\Psi_1(u)\rangle &= (-i)^2 (-1)^\xi \left[\frac{\theta_1(u + \frac{1}{4})}{\theta_1(u - \frac{1}{4})} \right]^2 |\Psi_1(u)\rangle, \\ \langle \Psi_1(u) | (T^2)^\dagger &= i^2 (-1)^\xi \left[\frac{\theta_1(u - \frac{1}{4})}{\theta_1(u + \frac{1}{4})} \right]^2 \langle \Psi_1(u) |. \end{aligned} \quad (\text{E9})$$

One can therefore conclude

$$\langle \Psi_1(u) | B_n | \Psi_1(u) \rangle = \langle \Psi_1(u) | B_{n+2} | \Psi_1(u) \rangle, \quad (\text{E10})$$

where B is an arbitrary operator. Analogously, one gets the following general identities

$$T^2 |\Psi_M(\mathbf{u})\rangle = (-1)^M (-1)^\xi e^{2i \sum_{l=1}^M p_l} |\Psi_M(\mathbf{u})\rangle, \quad (\text{E11})$$

$$\langle \Psi_M(\mathbf{u}) | B_n | \Psi_M(\mathbf{u}) \rangle = \langle \Psi_M(\mathbf{u}) | B_{n+2} | \Psi_M(\mathbf{u}) \rangle. \quad (\text{E12})$$

One can also check

$$\begin{aligned} T^N |\Psi_M(\mathbf{u})\rangle &= (-1)^{\frac{MN}{2}} (-1)^{\frac{N\xi}{2}} e^{Ni \sum_{l=1}^M p_l} |\Psi_M(\mathbf{u})\rangle \\ &= (-1)^{\frac{M(N+2)}{2}} (-1)^{(\frac{N}{2}+M)\xi} |\Psi_M(\mathbf{u})\rangle \\ &= |\Psi_M(\mathbf{u})\rangle. \end{aligned} \quad (\text{E13})$$

Due to the binary property of $\langle \sigma_n^z \rangle$, we only need to calculate the quantity $\langle \sigma_N^z \rangle$ and $\langle \sigma_{N-1}^z \rangle$. When $M = 1$, we have

$$\begin{aligned} \sigma_N^z |\kappa; n\rangle &= i^{N-1} |\kappa; n, N-1\rangle, \quad n \leq N-2, \\ \sigma_N^z |\kappa; N-1\rangle &= i |\kappa; N\rangle, \\ \sigma_N^z |\kappa; N\rangle &= -i |\kappa; N-1\rangle. \end{aligned} \quad (\text{E14})$$

Therefore, we get

$$\begin{aligned} \langle \Psi_1(u) | \sigma_N^z | \Psi_1(u) \rangle &= \frac{i}{2N} \sum_{\kappa=\pm 1} [\mathcal{A}_N(u)^* \mathcal{A}_{N-1}(u) \langle \kappa; N | \kappa; N \rangle - \mathcal{A}_{N-1}(u)^* \mathcal{A}_N(u) \langle \kappa; N-1 | \kappa; N-1 \rangle] \\ &= \frac{i}{N} \left[\frac{\theta_1(u - \frac{1}{4}) \theta_3(u - \frac{1}{4})}{\theta_1(u + \frac{1}{4}) \theta_3(u + \frac{1}{4})} - \frac{\theta_1(u + \frac{1}{4}) \theta_3(u + \frac{1}{4})}{\theta_1(u - \frac{1}{4}) \theta_3(u - \frac{1}{4})} \right] = \frac{1}{N} \mathcal{X}(u, +1). \end{aligned} \quad (\text{E15})$$

Using the same method, we have

$$\begin{aligned} \sigma_{N-1}^z |\kappa; n\rangle &= i^{N-1} |\kappa; n, N-1\rangle, \quad n \leq N-3, \\ \sigma_{N-1}^z |\kappa; N-2\rangle &= i |\kappa; N-1\rangle, \\ \sigma_{N-1}^z |\kappa; N-1\rangle &= -i |\kappa; N-2\rangle, \\ \sigma_{N-1}^z |\kappa; N\rangle &= i^{N-3} |\kappa; N-2; N-1\rangle, \end{aligned} \quad (\text{E16})$$

and

$$\langle \Psi_1(u) | \sigma_{N-1}^z | \Psi_1(u) \rangle = \frac{i}{N} \left[\frac{\theta_1(u - \frac{1}{4}) \theta_3(u + \frac{1}{4})}{\theta_1(u + \frac{1}{4}) \theta_3(u - \frac{1}{4})} - \frac{\theta_1(u + \frac{1}{4}) \theta_3(u - \frac{1}{4})}{\theta_1(u - \frac{1}{4}) \theta_3(u + \frac{1}{4})} \right] = \frac{1}{N} \mathcal{X}(u, -1). \quad (\text{E17})$$

For $M = 2$ case, the situation is slightly different. Let's first consider $\langle \Psi_2(\mathbf{u}) | \sigma_N^z | \Psi_2(\mathbf{u}) \rangle$ as an example. We know

$$\begin{aligned} \sigma_N^z |\kappa; n_1, n_2\rangle &= i^{N-1} |\kappa; n_1, n_2, N-1\rangle, \quad n_1 < n_2 \leq N-2, \\ \sigma_N^z |\kappa; n_1, N-1\rangle &= i |\kappa; n_1, N\rangle, \quad n_1 \leq N-2, \\ \sigma_N^z |\kappa; n_1, N\rangle &= -i |\kappa; n_1, N-1\rangle, \quad n_1 \leq N-2, \\ \sigma_N^z |\kappa; N-1, N\rangle &= (-i)^{N-1} |\kappa; N\rangle. \end{aligned} \quad (\text{E18})$$

Then, one can prove

$$\begin{aligned}
\langle \Psi_2(\mathbf{u}) | \sigma_N^z | \Psi_2(\mathbf{u}) \rangle &= 2i \sum_{n=1}^{N-2} [\chi_{n,N}(\mathbf{u})^* \chi_{n,N-1}(\mathbf{u}) - \chi_{n,N-1}(\mathbf{u})^* \chi_{n,N}(\mathbf{u})] \\
&= 2i \sum_{n=1}^N [\chi_{n,N}(\mathbf{u})^* \chi_{n,N-1}(\mathbf{u}) - \chi_{n,N-1}(\mathbf{u})^* \chi_{n,N}(\mathbf{u})] \\
&\stackrel{(C22)}{=} \frac{i}{N^2} \sum_{n=1}^N \sum_{j \neq l} [\mathcal{A}_n(u_j)^* \mathcal{A}_N(u_l)^* \mathcal{A}_n(u_j) \mathcal{A}_{N-1}(u_l) - \mathcal{A}_n(u_j)^* \mathcal{A}_{N-1}(u_l)^* \mathcal{A}_n(u_j) \mathcal{A}_N(u_l)] \\
&= \frac{1}{N} \sum_{l=1}^2 \mathcal{X}(u_l, +1).
\end{aligned} \tag{E19}$$

Using the same technique, we can prove Eq. (E2). \square

Appendix F: Two-point correlations

Define the following two-point operator

$$X_n = \sigma_n^x \sigma_{n+1}^y - \sigma_n^y \sigma_{n+1}^x. \tag{F1}$$

One can prove

$$\begin{aligned}
&\langle \Psi_M(\mathbf{u}) | T^\dagger X_n T | \Psi_M(\mathbf{u}) \rangle \\
&= \langle \Psi_M(\mathbf{u}) | Y^\dagger X_n Y | \Psi_M(\mathbf{u}) \rangle \\
&= \langle \Psi_M(\mathbf{u}) | X_n | \Psi_M(\mathbf{u}) \rangle,
\end{aligned} \tag{F2}$$

where

$$Y = \frac{1}{\sqrt{2^N}} \prod_{l=1}^{N/2} (\sigma_{2l-1}^x + \sigma_{2l-1}^y)(\sigma_{2l}^x - \sigma_{2l}^y), \quad Y^\dagger X_n Y = X_n. \tag{F3}$$

From Eqs. (E12) and (F2), we thus conclude

$$\langle \Psi_M(\mathbf{u}) | X_n | \Psi_M(\mathbf{u}) \rangle = \langle \Psi_M(\mathbf{u}) | X_m | \Psi_M(\mathbf{u}) \rangle. \tag{F4}$$

Without losing generality, we consider $\langle \Psi_M(\mathbf{u}) | X_1 | \Psi_M(\mathbf{u}) \rangle$. When $M = 1$, we have

$$\begin{aligned}
\sigma_1^x \sigma_2^y |\kappa; n\rangle &= |\kappa; n\rangle, \quad n \geq 2, \\
\sigma_1^x \sigma_2^y |\kappa; 1\rangle &= -|\kappa; 1\rangle, \\
\sigma_1^y \sigma_2^x |\kappa; n\rangle &= i^2 |-\kappa; 2, n\rangle, \quad 2 \leq n < N, \\
\sigma_1^y \sigma_2^x |\kappa; N\rangle &= (-i)^{N-2} |-\kappa; 2\rangle, \\
\sigma_1^y \sigma_2^x |\kappa; 2\rangle &= i^{N-2} |-\kappa; N\rangle, \\
\sigma_1^y \sigma_2^x |\kappa; 1\rangle &= -i^2 |-\kappa; 1, 2\rangle.
\end{aligned} \tag{F5}$$

Then, we can get

$$\langle \Psi_1(u) | \sigma_1^x \sigma_2^y | \Psi_1(u) \rangle = 1 - \frac{2\mathcal{A}_1(u)^* \mathcal{A}_1(u)}{N} = 1 - \frac{2}{N}, \tag{F6}$$

$$\langle \Psi_1(u) | \sigma_1^y \sigma_2^x | \Psi_1(u) \rangle = \frac{(-1)^\xi}{N} [\mathcal{A}_2(u)^* \mathcal{A}_N(u) + \mathcal{A}_N(u)^* \mathcal{A}_2(u)] = -\frac{\mathcal{Y}(u)}{N} - \frac{2}{N}, \tag{F7}$$

$$\langle \Psi_1(u) | X_1 | \Psi_1(u) \rangle = 1 + \frac{\mathcal{Y}(u)}{N}, \tag{F8}$$

where

$$\mathcal{Y}(u) = \left[\frac{\theta_1(u - \frac{1}{4})}{\theta_1(u + \frac{1}{4})} \right]^2 + \left[\frac{\theta_1(u + \frac{1}{4})}{\theta_1(u - \frac{1}{4})} \right]^2 - 2. \quad (\text{F9})$$

For $M \geq 2$ cases, we can use Eq. (C22) to prove

$$\langle \Psi_M(\mathbf{u}) | \sigma_1^x \sigma_2^y | \Psi_M(\mathbf{u}) \rangle = 1 - \frac{2M}{N}, \quad (\text{F10})$$

$$\langle \Psi_M(\mathbf{u}) | X_n | \Psi_M(\mathbf{u}) \rangle = 1 + \frac{1}{N} \sum_{l=1}^M \mathcal{Y}(u_l) = 1 - \frac{4}{N} \sum_{l=1}^M \sin^2 p_j. \quad (\text{F11})$$

We see that the two-point correlation $\langle \Psi_M(\mathbf{u}) | X_n | \Psi_M(\mathbf{u}) \rangle$ in the XY model is the same as that in the XX model.

Appendix G: The spin-helix eigenstate

For an XY model with $N = 4m$, $m \in \mathbb{N}^+$, we can construct the following states

$$\begin{aligned} |\Omega_1\rangle &= \frac{1}{\sqrt{2^N}} \bigotimes_{n=1}^N \begin{pmatrix} 1 \\ i^{n-1} \end{pmatrix}, \\ |\Omega_2\rangle &= \frac{1}{\sqrt{2^N}} \bigotimes_{n=1}^N \begin{pmatrix} 1 \\ i^{n+1} \end{pmatrix}, \\ |\Omega_3\rangle &= \frac{1}{\sqrt{2}} (|\Omega_1\rangle + |\Omega_2\rangle), \\ |\Omega_4\rangle &= \frac{1}{\sqrt{2}} (|\Omega_1\rangle - |\Omega_2\rangle). \end{aligned} \quad (\text{G1})$$

It can be proved that $|\Omega_{1,2,3,4}\rangle$ are all eigenstates of the Hamiltonian. The magnetization profiles in the aforementioned states are

$$\begin{aligned} \langle \sigma_{2l}^x \rangle_{1,2} &= 0, \quad \langle \sigma_{2l+1}^x \rangle_1 = (-1)^l, \quad \langle \sigma_{2l+1}^x \rangle_2 = (-1)^{l+1}, \\ \langle \sigma_{2l+1}^y \rangle_{1,2} &= 0, \quad \langle \sigma_{2l}^y \rangle_1 = (-1)^{l+1}, \quad \langle \sigma_{2l}^y \rangle_2 = (-1)^l, \\ \langle \sigma_l^z \rangle_{1,2,3,4} &= \langle \sigma_l^x \rangle_{3,4} = \langle \sigma_l^y \rangle_{3,4} = 0. \end{aligned} \quad (\text{G2})$$

One can also get the two-point correlation under the states $|\Omega_{1,2,3,4}\rangle$

$$\langle X_l \rangle_{1,2,3,4} = 1. \quad (\text{G3})$$

Appendix H: XX limit

Since the chiral basis vector $|\pm 1; \mathbf{n}\rangle$ is the same for both the XX model and the XY model, all the calculation techniques domesticated in the appendices also work for the XX model. The only difference is that the binary factors $\left[\frac{\theta_3(u_l + \frac{1}{4})}{\theta_3(u_l - \frac{1}{4})} \right]^{\pm \frac{1}{2}}$ exist in the XY chain, while they will disappear in the XX case.

It should be noted that the direct reduction of the XY model to the XX model may yield results different from those presented in Table II.

When $\tau \rightarrow +i\infty$, the XY model degenerates into XX model with $J_{x,y} \rightarrow 1$. For a large τ , most of the Bethe roots are finite. In contrast, two Bethe roots exhibit significantly large values

$$u_l = \frac{\tau}{2}, \frac{1 - \tau}{2}. \quad (\text{H1})$$

In the XX limit, for the finite Bethe roots, we see that

$$\theta_3(u_l \pm \frac{1}{4}) = 1, \quad \mathcal{A}_n(u_l) = e^{inp_l}, \quad (\text{H2})$$

which is consistent with Theorem 2. The quantities $\mathcal{X}(u_l, \pm 1)$ for finite u_l read

$$\mathcal{X}(u_l, +1) = \mathcal{X}(u_l, -1) = i(e^{-ip_l} - e^{ip_l}) = 2 \sin p_l. \quad (\text{H3})$$

For the remaining two infinite roots: $u_l = \frac{\tau}{2}, \frac{1-\tau}{2}$, the function $\mathcal{A}_n(u_l)$ has the following form

$$\mathcal{A}_n(\frac{\tau}{2}) = \frac{(-i)^n - i^{n+1}}{\sqrt{2}}, \quad \mathcal{A}_n(\frac{1-\tau}{2}) = \frac{i^n + (-i)^{n+1}}{\sqrt{2}}. \quad (\text{H4})$$

In the limit $\tau \rightarrow +i\infty$, the direct reduction of the chiral Bethe state in Theorem 3 will yield recombined eigenstates instead of the chiral Bethe states in Theorem 2 when $\frac{\tau}{2}$ or $\frac{1-\tau}{2}$ is included in the Bethe root set $\{u_1, \dots, u_M\}$. One can also prove that

$$\mathcal{X}(\frac{\tau}{2}, \pm 1) = \mathcal{X}(\frac{1-\tau}{2}, \pm 1) = 0, \quad \mathcal{Y}(\frac{\tau}{2}) = \mathcal{Y}(\frac{1-\tau}{2}) = -4. \quad (\text{H5})$$

Appendix I: Proof of (17)

We introduce the fermionic partition sum

$$Z = \prod_p (1 + e^{hj_p + \mu}), \quad (\text{I1})$$

where μ and h are chemical potentials for the “particle number” M and the current J respectively. Denoting $\Phi = \ln Z$ and differentiating w.r.t. μ we get a relation between M and μ , namely,

$$M = \left. \frac{\partial \Phi}{\partial \mu} \right|_{h=0} = N \partial_\mu \ln(1 + e^\mu), \quad (\text{I2})$$

leading to

$$\frac{M}{N} = \frac{1}{1 + e^{-\mu}}. \quad (\text{I3})$$

The average current \bar{J} is given analogously by differentiating Φ w.r.t. h , using $j_p = 2 - 8 \sin^2 p$ (see last line of Table I) and substituting (I3), leading to

$$\bar{J} = 2N - 4M. \quad (\text{I4})$$

Finally, to obtain the variance of the current for fixed M , we need $\partial_h^2 \Phi$ for fixed M , or $\partial_h J$ for fixed M . This is obtained via use of standard thermodynamic relations

$$\langle (J - \bar{J})^2 \rangle_M = \left(\frac{\partial J}{\partial h} \right)_M = \frac{\partial(J, M)}{\partial(h, M)} = \frac{\partial(J, M)}{\partial(h, \mu)} \frac{\partial(h, \mu)}{\partial(h, M)} \quad (\text{I5})$$

$$= \left[\left(\frac{\partial J}{\partial h} \right)_\mu \left(\frac{\partial M}{\partial \mu} \right)_h - \left(\frac{\partial J}{\partial \mu} \right)_h \left(\frac{\partial M}{\partial h} \right)_\mu \right] \left(\frac{\partial \mu}{\partial M} \right)_h \quad (\text{I6})$$

$$= \partial_h^2 \Phi - \frac{(\partial_h \partial_\mu \Phi)^2}{\partial_h^2 \Phi}. \quad (\text{I7})$$

After some algebra, we obtain the thermodynamic result

$$\langle (J - \bar{J})^2 \rangle_M = 8M \left(1 - \frac{M}{N} \right). \quad (\text{I8})$$

which is valid in the thermodynamic limit of large N and fixed M/N . However finite-size corrections exist as shows a comparison of (I8) with the exact formula for $M = 1$

$$\langle (J - \bar{J})^2 \rangle_1 = \langle (-8 \sin^2 p_1 + 4)^2 \rangle = 4^2 \langle \cos^2 2p_1 \rangle = 8, \quad (\text{I9})$$

suggesting a slight modification of (I8)

$$\langle (J - \bar{J})^2 \rangle_M = 8M \frac{1 - \frac{M}{N}}{1 - \frac{1}{N}}, \quad (\text{I10})$$

i.e. (17). Comparison of the above with exact numerics for sizes $N \leq 24$ and arbitrary M strongly suggests that (17) provides the exact expression for the variance of the current for any M, N .

For the S^z eigenbasis, with $j_k = 8 \sin k$, the analogous investigation yields the average current and variance for fixed magnetization $S^z = M - N/2$

$$\bar{J} = 0, \quad \langle (J - \bar{J})^2 \rangle_M = 32M \frac{1 - \frac{M}{N}}{1 - \frac{1}{N}}. \quad (\text{I11})$$